JMEPEG (2009) 18:511–516
DOI: 10.1007/s11665-009-9357-2

1059-9495/$19.00

Properties and Heat Treatment of High Transition Temperature Ni-Ti-Hf Alloys

C. Craig Wojcik

(Submitted September 11, 2008; in revised form November 21, 2008)

The high transition temperature Ni-Ti (Hf, Zr) alloys have long been of interest for actuators and other applications requiring transition temperatures greater than 100 °C. Unfortunately, the high hardness and poor fabricability of these alloys have prohibited the scale up to commercial production. Some of these alloys are so "hot short" that even modest size ingots cannot be cast without internal cracks formed by solidification shrinkage stresses. Hot rolling methods have recently been demonstrated that can produce crack free Ni-Ti-(6-10 at.%)Hf thin sheets having austenite transition temperatures up to approximately 170 °C. Since these alloys are soft martensite phase at room temperature, they can easily be formed and bent at ambient temperature but cold rolling can only be performed to a limited extent due to high work hardening rates which are typical for Ni-Ti alloys. Progress is now underway to scale up these methods to produce 500-600 mm wide sheets. The effects of composition variations, heat treatment and cold working on transition temperatures are discussed. Microstructural features unique to these ternary alloys and impurity effects are also discussed. The effects of stress on transition temperature have been determined. Austenite transition temperatures, as measured by DSC and bend-free recovery testing, can be controlled within 100-170 °C for these alloys.

Keywords aerospace, biomaterials, intermetallics, refractory metals, titanium

1. Introduction

Binary NiTi alloys have a long history of use as superelastic and shape memory components. The martensite to austenite transformation temperature range possible with these alloys is very useful since it can be tailored from well below room temperature to about 100 °C. Combinations of very controlled Ni/Ti ratio and thermo-mechanical treatments are routinely used to control the exact transformation temperature within just a few degrees. Additionally, these alloys can be made slightly nickel rich to allow precipitation of Ni_4Ti_3 type particles to further enhance strength and shape stability. Unfortunately, these materials cannot be used in applications as a shape memory actuator where operating environments are not cold enough to induce a return back to the martensite phase. An example of this would be in or near an internal combustion or turbine engine compartment. In other potential applications, it may take too long for an actuator to cool to the maximum martensite transformation temperature obtainable with conventional NiTi alloys. This would result in the actuator having too long of a response time. For these reasons, many researchers have tried to develop substantially higher temperature shape memory alloys. The most alluring of these possible alloys have been Ni-Ti-X alloys. The third X component of which can be Hf, Zr, Pd, or Pt. Austenite transformations temperatures of 300-400 °C have been well documented for these alloys yet none have ever approached commercial status (Ref 1-3). Aside from the cost considerations of Hf, Pd, and Pt, all these alloys suffer from very poor hot fabricability, and deficient mechanical properties compared to normal NiTi alloys. The properties of these alloys have often been reported on very small pieces of cast material with little or no hot and cold working to homogenize and refine the grain structure. Conventional NiTi binary alloys must always be hot worked to obtain acceptable shape memory properties. For this reason, it is believed that some data reported on these ternary alloys may be far from optimum data obtainable on a well-refined wrought type structure.

From the group of previously mentioned ternary additions, Hf, Zr, Pt, and Pd, researchers at ATI Wah Chang have always been interested in Ni-Ti-Hf system because it is much more economical than Pt or Pd and it affects the transformation temperature more strongly than Zr for a given increase in alloy substitution. Both Hf and Zr substitute directly for the Ti atoms in the NiTi lattice structure. In 1994, Tuominen (Ref 4) reported on attempts to fabricate Ni-Ti alloys containing 8-16 at.% Hf. Even the relatively modest 10% Hf alloy proved very difficult to fabricate. Even more disappointing was a reported very low percentage of recovered strain, only 0.44% at a test stress of 138 MPa. Later attempts to fabricate Ni-40Ti-10Hf material by high temperature extrusion proved that fabricability was still a major problem that could not be easily resolved. The resultant extrusion from this work (Ref 5) is

This article is an invited paper selected from presentations at Shape Memory and Superelastic Technologies 2008, held September 21-25, 2008, in Stressa, Italy, and has been expanded from the original presentation.

C. Craig Wojcik, ATI Wah Chang, an Allegheny Technologies Company, Albany, OR 97321. Contact e-mail: craig.wojcik@wahchang.com.

shown in Fig. 1. Enthusiasm for that alloy system waned and further work was discontinued. More recently, that alloy system was revisited in 2006. By 2006, additional processing knowledge had been gained from learning how to make higher purity Ni-Ti alloys and learning how to manufacture a much more challenging Ni-40Ti alloy that previously could not be fabricated. That work, which led to a lab scale process capable of making crack free Ni-40Ti-10Hf sheets, formed the basis of this study (Ref 6). Some of the early unsuccessful attempts and later successfully rolled buttons are shown in Fig. 2.

Fig. 1 Ni-40Ti-10Hf Extrusion attempt, unpublished research (Ref 5) at ATI Wah Chang

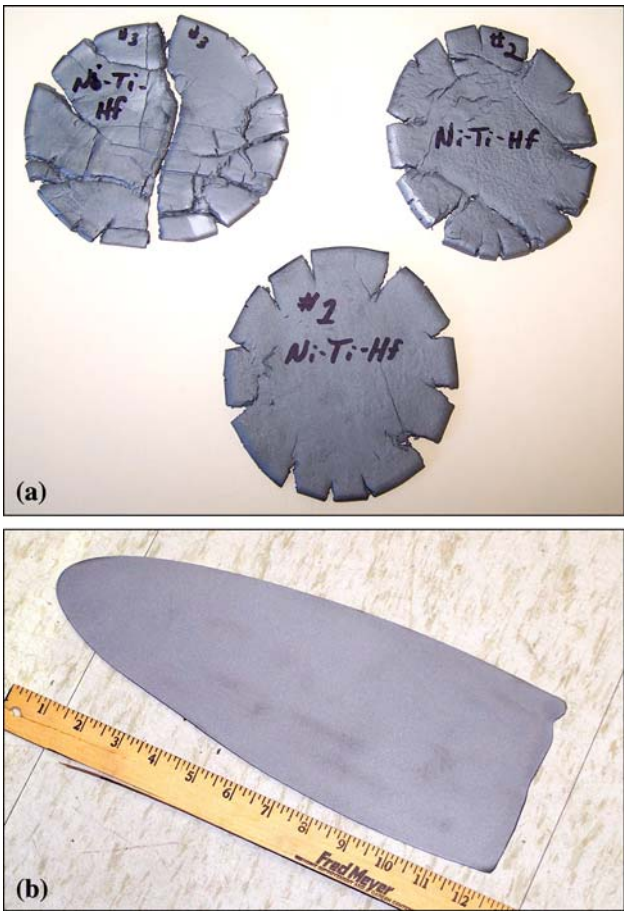

Fig. 2 Preliminary attempts to hot roll Ni-40Ti-10Hf arc melted buttons encased in steel cans (a), and successfully hot-rolled button 0.6 mm thick (b) (Ref 6)

2. Material Preparation

A total of five alloys were made into thin test sheets to investigate the effects of oxygen content and hafnium concentration. All alloys were melted into buttons approximately 10 mm thick × 70 mm in diameter using the nonconsumable vacuum arc melting method with a water-cooled copper mold. Each alloy was melted at least five times to obtain sufficient mixing of the alloy ingredients. The raw materials used included high-purity electrolytic nickel plate, iodide crystal titanium, and commercial purity hafnium sheet. Initially, it was expected that these high-purity ingredients would be essential for obtaining sufficient hot workability. After hot rolling success was achieved, then commercial purity Grade I titanium sheet was used for the lower purity buttons. The faces of the buttons were machined to remove any laps and then welded in steel cans for hot rolling. The cans provided a greater thermal mass to keep the buttons uniformly hot during rolling and allow hot rolling to a thinner cross section.

After rolling, the sheets were grit blasted, and then chemically cleaned in a mixture of 50% HNO_3 and 25% HF, balance water. Samples for aging heat treatment were cut to ~1 cm wide × 8 cm long. Samples for constant load dilatometry (CLD) were sheared with a shaped punch and die directly into the tensile testing configuration with a gage section measuring 6.35 mm wide × 76.2 mm long. One of the hot-rolled sheets is shown in Fig. 3 with one of the CLD test specimens. The tensile axis of these samples corresponded to the rolling direction. Prior to any heat treatment, the samples were wrapped in titanium foil and sealed in helium backfilled quartz capsules. All heat-treated samples were cooled immediately by water quenching the capsules. The 1 × 8 cm sample strips were used for bend-free recovery (BFR) testing, metallographic samples, and differential scanning calorimetry (DSC). Austenite start and finish temperatures were measured with the BFR method using a bending mandrel that produced a surface strain of 3% after cooling in liquid nitrogen. The 5 mm diameter samples for DSC testing were punched directly out of the heat-treated sheets and then pickled in acid to remove 20-40 μm of surface metal. A scan rate of 10 °C per min was used for all DSC tests.

Fig. 3 Hot-rolled Ni-40Ti-10Hf sheet 0.6 mm thick showing CLD transformation test samples punched out at room temperature. Overall sample length is 16 × 1.7 cm wide at grip section

Austenite and martensite transition temperatures measured with the CLD method were determined while under a constant tensile stress of 138 and 276 MPa (20 and 40 ksi). In this test, the specimen was initially heated above the austenite finish temperature (250-300 °C) and then a static tensile load was applied with weights. A metal pipe wrapped with heat tape surrounded the specimen and full length of the grips to maintain temperature uniformity. The temperature was lowered past the martensite finish temperature and then raised well above the austenite finish temperature while the strain was continuously measured. The CLD tests were conducted as a series of three consecutive tests on the same sample to see how reproducibly the strain was recovered after a second cycle at 138 MPa. Then on the third cycle, the stress was increased to 276 MPa to see how much the transformation temperatures, and strain would increase at a higher stress.

3. Material Evaluation and Discussion

Chemical analysis of the alloys was obtained on samples of the sheet after hot rolling and acid cleaning. These results summarized in Table 1 show good agreement between the target and measured compositions. Buttons #1 and #2 had the lowest oxygen content compared with the other three alloys that were made with lower purity Grade 1 titanium sheet.

Microstructural samples were examined after hot rolling, quenching, and aging heat treatments. Using light microscopy, the effects of heat treatment could not be seen in the structure. These structures are shown in Fig. 4. The martensite platelets and second-phase particles are clearly visible in all the alloys. A greater concentration of second-phase particles was seen in the alloys with higher oxygen concentration. The alloy with only 6% Hf had a noticeably finer martensite structure. That alloy also had the highest level of carbon and oxygen impurities.

Second-phase particles in conventional binary Ni-Ti alloys made by arc melting contain a complex Ti_4-Ni_2-O_x lower oxide phase (Ref 7) so it is assumed that a similar oxygen rich phase is present in these alloys however, it may be even more stabilized by the hafnium content. These particles must be substantially harder than the matrix at rolling temperatures since they do not exhibit the long aspect ratio expected from the degree of rolling deformation performed on the buttons. We attempted to perform a quantitative SEM analysis on that phase; however, the small size of the particles limited our precision. Images of these particles in the backscattered SEM detection mode are shown in Fig. 5, along with the spectrum obtained in Fig. 6. There is a slight indication that the particles have a higher concentration of titanium and a lower concentration of hafnium and nickel than the matrix.

After hot rolling and cleaning, the samples were heat treated by either a high temperature anneal or low temperature aging treatment. The annealing heat treatments of 900 and 950 °C were carried out for a time of 60 min. Samples of the alloys were aged at 500-600 °C for several time periods up to 120 h. These samples were then tested with the DSC to see what effects aging had on the austenite and martensite transition temperatures. These results for the 10% hafnium alloy after aging 120 h are shown in Fig. 7 and after 72 h for the 6%

Table 1 Analysis of Ni-Ti-Hf alloy sheets hot rolled to 0.6 mm thick

Alloy element	$Ni_{50}Ti_{40}Hf_{10}$ (44.2Ni-28.9Ti-26.9Hf wt.%), Button #1	$Ni_{50}Ti_{40}Hf_{10}$ (44.2Ni-28.9Ti-26.9Hf wt.%), Button #2	$Ni_{50}Ti_{40}Hf_{10}$ (44.2Ni-28.9Ti-26.9Hf wt.%), Button #3	$Ni_{50}Ti_{42}Hf_{8}$ (46.0Ni-31.6Ti-22.4Hf wt.%), Button #4	$Ni_{50}Ti_{44}Hf_{6}$ (48.0Ni-34.5Ti-17.5Hf wt.%), Button #5
Hafnium	26.70 wt.%	26.92	26.86	21.80	17.0
Nickel	44.27 wt.%	44.21	44.12	46.70	49.77
Oxygen	110 wppm	150	310	240	410
Nitrogen	<20 wppm	<20	25	20	31
Hydrogen	50 wppm	24	22	20	23
Carbon	45 wppm	32	43	50	76

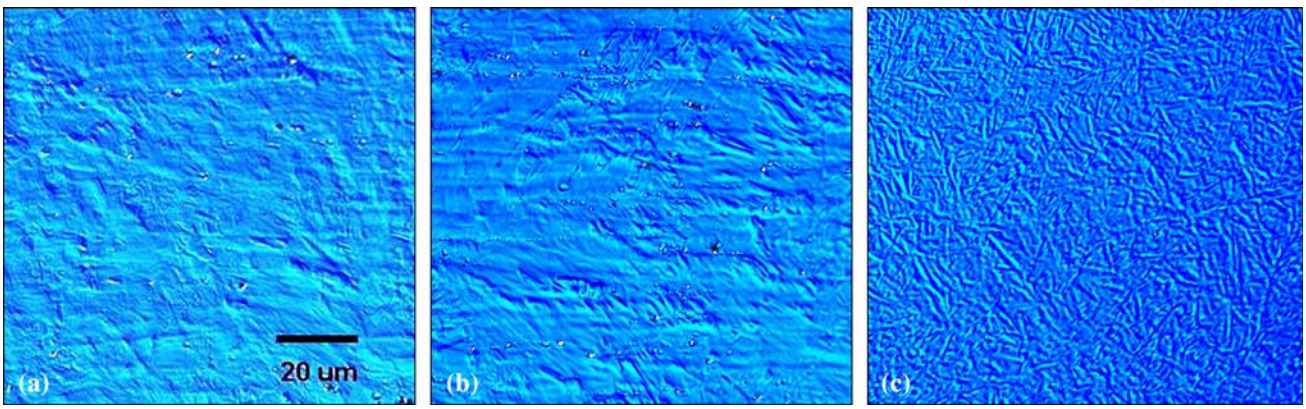

Fig. 4 Microstructure of alloy sheets after hot rolling and quenching. (a) 10% Hf 150 ppm oxygen, (b) 10% Hf 310 ppm oxygen, and (c) 6% Hf 410 ppm oxygen, longitudinal sections

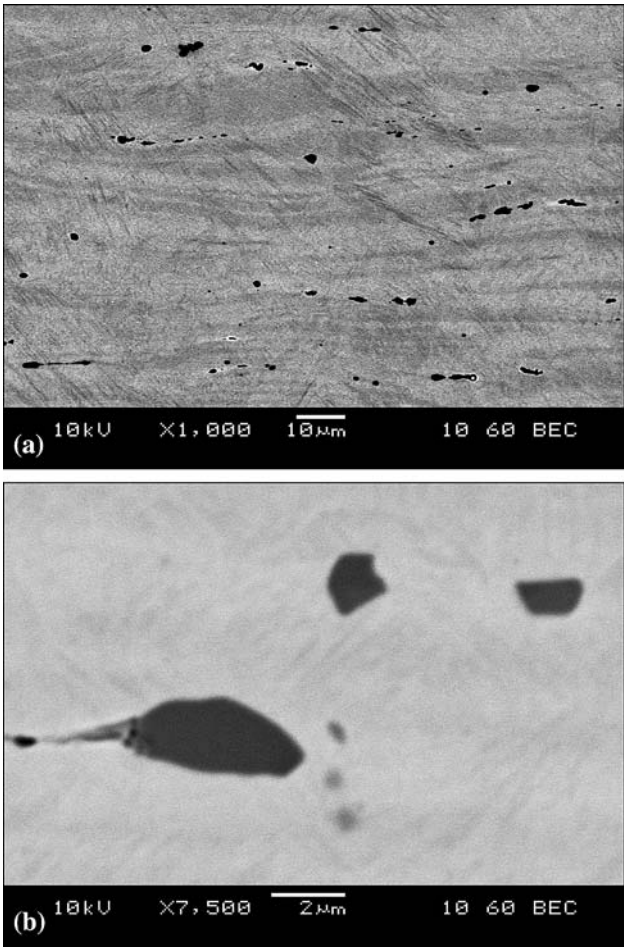

Fig. 5 Backscattered images of second-phase particles observed in the 10% Hf alloy sheet containing 310 ppm oxygen, longitudinal section

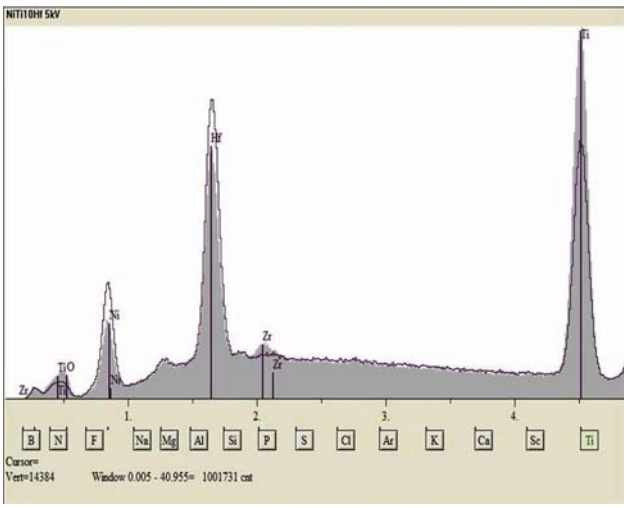

Fig. 6 SEM qualitative composition analyses of second-phase and matrix phase. Line is matrix, gray-shaded area is second-phase particle

hafnium alloy in Fig. 8. Although we observed some minor temperature shifts and reshaping of phase transition peaks, there was no major shift in the transition temperatures. This was

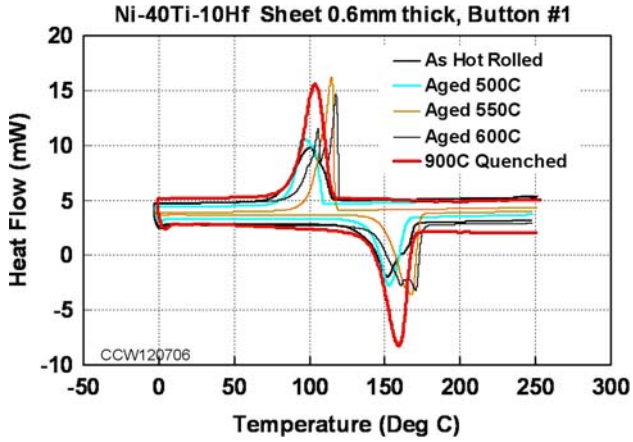

Fig. 7 DSC test results after various aging and quenching heat treatments of the 10% Hf alloy

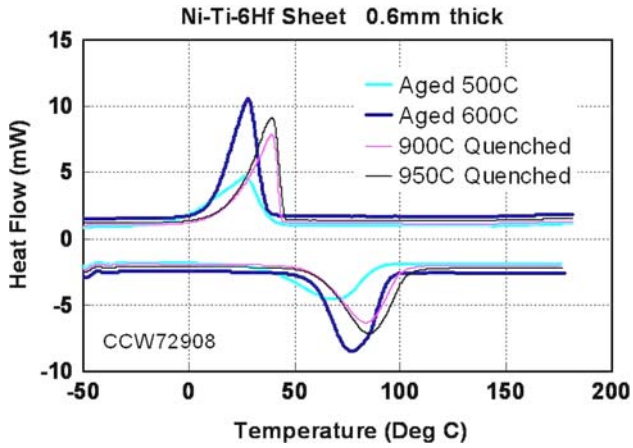

Fig. 8 DSC test results after various aging and quenching heat treatments of the 6% Hf alloy

a good indication that these alloys did not contain a significant excess of nickel. When excess (i.e., supersaturated) nickel is present, it typically will precipitate out as Ni_4Ti_3 type lenticular-shaped precipitates during aging (Ref 8-10). This lowers the nickel concentration in the matrix which results in increases in the transition temperatures after aging. Since aging heat treatments appeared to have only a minor affect on these alloys an anneal/quench heat treatment of 60 min at 900 °C was used on all the subsequent test samples.

The effects of oxygen on the 10% Hf alloy are shown in Fig. 9 with all the alloys in the quenched heat treatment. It should be noted that the martensite peak for the alloy containing 150 ppm oxygen has an initial spike that should not be confused with an R phase peak. This is a testing artifact that is usually attributable to poor thermal coupling to the DSC test pan. The transition temperatures are shown for the various oxygen levels after being aged for 120 h at 650 °C in Table 2. A temperature decrease of about 20° was noted for the 310 ppm oxygen level with both heat treatments. Since it is not precisely known what the composition ratio of Ni to Ti and Hf is in the second-phase particles, this shift in transition temperature could be simply a result of oxygen rich second-phase particles shifting the metal alloy ratio rather than an intrinsic effect of lower oxygen dissolved in the matrix phase.

The effect of hafnium concentration on transition temperatures is shown in Fig. 10 for buttons 2, 4, and 5. All these alloys display sharp and symmetrical transition peaks with approximately 60 °C hysteresis between the austenite and martensite peaks.

Results of CLD testing the 6% Hf alloy are shown in Fig. 11. This alloy displays very consistent recoverable strain for both the first and second cycle at 138 MPa. At 276 MPa, the total strain increased only about 1% which indicates a high rate of strain hardening in the martensite. Approximately 5.5 of the total 6% strain was recovered in that alloy when heated back to the austenite phase. It is expected that after more cycles at 276 MPa the total strain would decrease and the percentage of strain recovery would increase. Both the martensite and austenite transformation temperatures increase with stress, approximately 20 °C for 276 MPa compared to 138 MPa.

CLD test results for the 10% Hf alloy with low (150 ppm) and high (310 ppm) oxygen are shown in Fig. 12 and 13. These

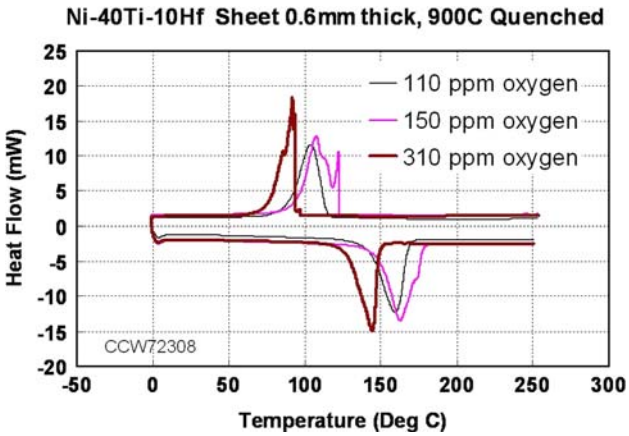

Fig. 9 DSC test results for various levels of oxygen in 10% Hf alloy sheet

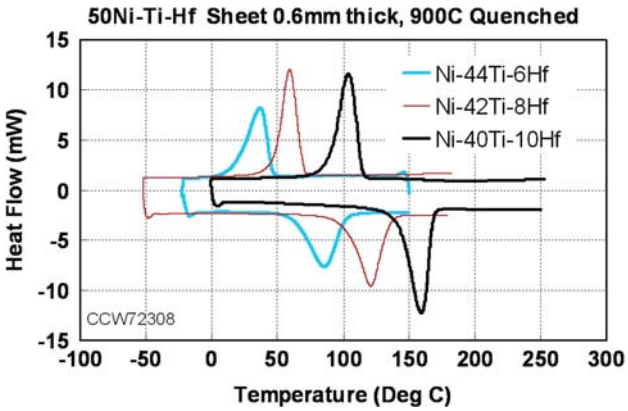

Fig. 10 DSC scans for various concentrations of hafnium

Table 2 Transformation temperatures as measured by bend-free recovery method for various oxygen levels, quenched, and aged heat treatments

$Ni_{50}Ti_{40}Hf_{10}$ bend-free recovery austenite transition temperature				
	A_s, °C		A_f, °C	
Oxygen concentration, wppm	He quenched 900 °C, 60 min	Aged 600 °C, 120 h	He quenched 900 °C, 60 min	Aged 600 °C, 120 h
110	188	184	196	195
150	188	178	197	193
310	164	157	174	169

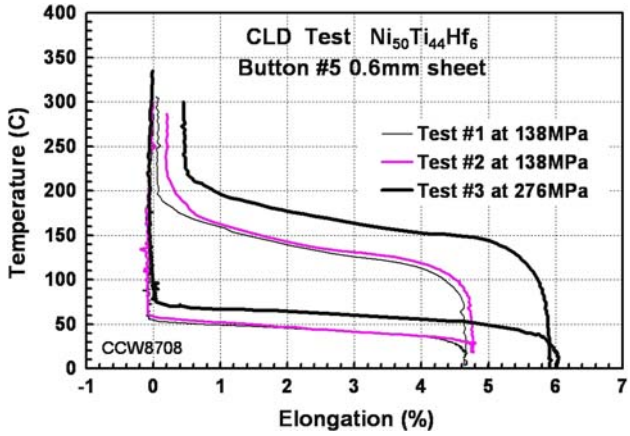

Fig. 11 CLD test results for 6% Hf alloy sheet

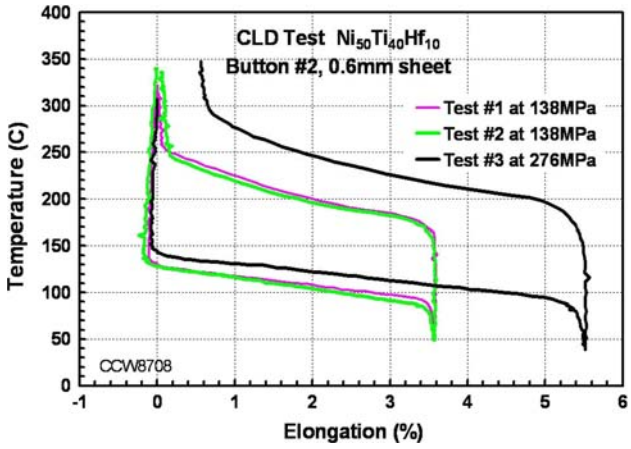

Fig. 12 CLD test results for 10% Hf, 150 ppm oxygen sheet

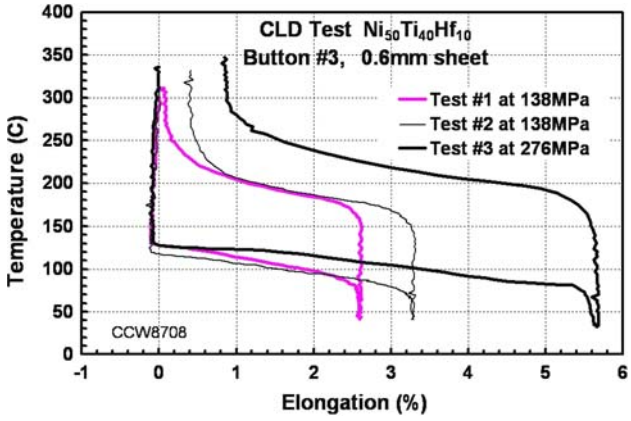

Fig. 13 CLD test results for 10% Hf, 310 ppm oxygen sheet

Table 3 Summary of CLD test transition temperatures and recovered energy

	Summary of CLD transition temperatures					
Alloy button	**Stress, MPa**	A_s, °C	A_f, °C	M_s, °C	M_f, °C	**Recovered energy, J/cm^3**
Ni-44Ti-6Hf, Button #5	138 test #1	95	175	58	33	6.2
	138 test #2	97	172	53	36	6.2
	276 test #3	124	199	74	47	15.2
Ni-40Ti-10Hf, Button #2	138 test #1	159	250	129	91	4.8
	138 test #2	158	239	130	86	4.8
	276 test #3	174	275	141	91	13.8
Ni-40Ti-10Hf, Button #3	138 test #1	169	224	134	87	3.5
	138 test #2	161	216	121	77	4.1
	276 test #3	175	256	140	74	13.5

alloys show similar results to the 6% Hf alloy; however, the transitions temperatures are all shifted higher and the total strains are lower as would be expected for a martensite phase with a higher yield strength. The first cycle at 138 MPa on the specimen from button #3 had an unusually low strain. This may be a result of bending damage during fixture assembly. At room temperature, the 0.6-mm-thick martensite samples can very easily be bent during handling.

All of the CLD data are summarized in Table 3. Additionally a calculation was made to determine how much recoverable energy was observed for each test condition. At lower stress, 138 MPa, the 6% Hf alloy had the highest energy recovery due to the increased strain compared to the 10% Hf alloys. The highest recovered energy for all alloys was at the highest stress, 276 MPa, which produced more recoverable strain. The maximum energy value of 15.2 J/cm^3 for the 6% Hf alloy at 276 MPa is a very high value for any shape memory metal. It compares favorably even with cold worked conventional NiTi alloy sheet as measured in the same CLD test in a previous study (Ref 8), and cold worked and aged commercially available SM495 wire (Ref 11).

4. Conclusions

In summary, we have shown that the Ni-Ti-Hf system can be processed to yield useful shape memory properties with high recovery strains and high recovery energy. Hafnium additions up to 10% can be used to enhance the austenite transition temperature almost 100 °C higher than conventional Ni-Ti alloys. The effects of changes in oxygen level and hafnium content have been further documented at zero stress and two levels of constant tensile stress. Additional testing needs to be completed to determine the shape memory properties after many cycles, as well as the superelastic properties of these alloys which should occur at elevated temperatures of 100 °C or more. Ongoing work to scale up the processing size capability for this family of alloys however will determine if these compositions can become a commercial success.

References

1. D.N. AbuJudom, P.E. Thoma, Ming-Yuan Kao, and D.R. Angst, U.S. Patent 5,114,504
2. P.G. Lindquist and C.M. Wayman, Shape Memory and Transformation Behavior of Martensitic Ti-Pd-Ni and Ti-Pt-Ni Alloys, in *Engineering Aspects of Shape Memory Alloys*, T.W. Durig, K.N. Melton, D. Stockel, and C.M. Wayman, Eds., Butterworth-Heinemann, Boston, 1990, p 58–68
3. D. Goldberg, Y. Xu, Y. Murakami, S. Morito, K. Otsuka, T. Ueki, and H. Horikawa, Improvement of a $Ti_{50}Pd_{30}Ni_{20}$ High Temperature Shape Memory Alloy by Thermomechanical Treatments, *Scripta Metall. Mater.*, 1994, **30**, p 1349–1354
4. S.M. Tuominen, High Temperature Ni-Ti-Hf Alloys, *SMST-1994*, A.R. Pelton, D. Hodgson, and T. Durig, Eds., MIAS, Monterey, 1995, p 49–54
5. S.M. Tuominen, Unpublished Research, ATI Wah Chang, 1994
6. C.C. Wojcik, Unpublished Research, ATI Wah Chang, 2006
7. *Standard Specification for Wrought Nickel-Titanium Shape Memory Alloys for Medical Devices and Surgical Implants*, ASTM Standard F 2063-05, ASTM International, West Conshohocken, 1995
8. C.C. Wojcik, Aging Effects in Nickel Rich Ni-Ti Alloys, *SMST-2004*, M. Mertmann, Ed., ASM International, Materials Park, 2006, p 229–236
9. R.J. Wasilewski, S.R. Butler, J.E. Hanlon, and D. Worden, *Met. Trans.*, 1971, **2**, p 229–238
10. M. Nishida, C.M. Wayman, and T. Honma, *Met. Trans.*, 1986, **17A**, p 1505–1515
11. R. Noebe, D. Gaydosh, S. Padula II, A. Garg, T. Biles, and M. Nathal, Properties and Potential of Two (Ni,Pt)Ti Alloys for use as High-Temperature Actuator Materials, *Smart Structures and Materials 2005, Proceedings of SPIE 5761*, W.D. Armstrong, Ed., International Society for Optical Engineering, Bellingham, 2005, p 364–375